crust-mantle decoupling, volcanism and basin formation: a new model for the Pliocene-Quaternary evolution of the southern East-Carpathians, Romania. *Tectonophysics* **327**, 83–107 (2000).

20. James, D. E. & Sacks, I. S. in *Geology and Ore Deposits of the Central Andes* Spec. Pub. 7 (ed. Skinner, B. J.) 1–25 (Society of Economic Geologists, Littleton, Colorado, 1999).

21. Owens, T. J. & Zandt, G. Implications of crustal property variations for models of Tibetan plateau evolution. *Nature* **387**, 37–43 (1997).

22. Mahdi, H. & Pavlis, G. L. Velocity variations in the crust and upper mantle beneath the Tien Shan inferred from Rayleigh wave dispersion: Implications for tectonic and dynamic processes. *J. Geophys. Res.* **103**, 2693–2703 (1998).

23. Hacker, B. R. *et al.* Hot and dry deep crustal xenoliths from Tibet. *Science* **287**, 2463–2466 (2000).

24. Forsyth, D. W. Subsurface loading and estimates of the flexural rigidity of the continental lithosphere. *J. Geophys. Res.* **90**, 12623–12632 (1985).

25. Stewart, J. & Watts, A. B. Gravity anomalies and spatial variations of flexural rigidity at mountain ranges. *J. Geophys. Res.* **102**, 5327–5352 (1997).

26. McKenzie, D. & Fairhead, D. Estimates of the effective elastic thickness of the continental lithosphere from Bouguer and free air gravity anomalies. *J. Geophys. Res.* **102**, 27523–27552 (1997).

27. Djomani, Y. H. P., Fairhead, J. D. & Griffin, W. L. The flexural rigidity of Fennoscandia: reflection of the tectonothermal age of the lithospheric mantle. *Earth Planet. Sci. Lett.* **174**, 139–154 (1999).

28. Döring, J. & Götze, J.-J. The isostatic state of the southern Urals crust. *Geol. Rundsch.* **87**, 500–510 (1999).

29. Hittelman, A. M., Kinsfather, J. O. & Meyers, H. *Geophysics of North America* [CD-ROM] (National Geophysical Data Center, Boulder, CO, 1990).

30. Rudnick, R. L. & Fountain, D. M. Nature and composition of the continental crust: a lower crustal perspective. *Rev. Geophys.* **33**, 267–309 (1995).

31. Christensen, N. I. & Mooney, W. D. Seismic velocity structure and composition of the continental crust: A global view. *J. Geophys. Res.* **100**, 9761–9788 (1995).

32. Hacker, B. R. in *Subduction Top to Bottom* Geophysical Monograph 96 (eds Pakiser, L. C. & Mooney, W. D.) 337–346 (American Geophysical Union, Washington DC, 1996).

Bird-like fossil footprints from the Late Triassic

Ricardo N. Melchor*†, **Silvina de Valais**‡ & **Jorge F. Genise***‡

* CONICET & † Universidad Nacional de La Pampa, Av. Uruguay 151, 6300 Santa Rosa, La Pampa, Argentina
‡ Museo Paleontológico "Egidio Feruglio", Av. Fontana 140, 9100 Trelew, Chubut, Argentina

The study of fossilized footprints and tracks of dinosaurs and other vertebrates has provided insight into the origin, evolution and extinction of several major groups and their behaviour; it has also been an important complement to their body fossil record[1–4]. The known history of birds starts in the Late Jurassic epoch (around 150 Myr ago) with the record of *Archaeopteryx*[5], whereas the coelurosaurian ancestors of the birds date back to the Early Jurassic[6]. The hind limbs of Late Triassic epoch theropods lack osteological evidence for an avian reversed hallux and also display other functional differences from birds[7]. Previous references to suggested Late Triassic to Early Jurassic bird-like footprints have been reinterpreted as produced by non-avian dinosaurs having a high angle between digits II and IV[8,9] and in all cases their avian affinities have been challenged[10]. Here we describe well-preserved and abundant footprints with clearly avian characters from a Late Triassic redbed sequence of Argentina[11,12], at least 55 Myr before the first known skeletal record of birds. These footprints document the activities, in an environment inter-

preted as small ponds associated with ephemeral rivers, of an unknown group of Late Triassic theropods having some avian characters.

Numerous small, bird-like footprints (Fig. 1) were discovered in, and collected from, the middle part of the Late Triassic Santo Domingo formation[13] from northwest Argentina, La Rioja Province (28° 32′ S, 68° 45′ W). The age of the unit has been established on the basis of its fossil content and a radiometric date, and is further supported by lithologic comparison with the well-dated Late Triassic Los Colorados formation[11]. The unit at the studied locality has produced remains of *Rhexoxylon*[11], a wood morphogenus only reported from Middle to Late Triassic rocks of Gondwana[14]. Concurrently, an interbedded basalt flow located about 80 m above the track-bearing horizons yielded an ^{40}Ar/^{39}Ar plateau age of 212.5 ± 7.0 Myr ago (step-heating analysis on albite crystal)[12], which suggests a Norian–Rhaetian age for the basalt according to recent calibrations of the Triassic–Jurassic timescale[15–17]. The tracks occur in two trampled bedding planes (each up to 1.9 square metres) having a vertical spacing of less than 10 cm. Footprints appear with variable density and quality of preservation on the worked bedding planes (Fig. 1a); they are better preserved in the lower horizon, both as natural casts and moulds. In its central part (composed of claystone) they exhibit a high density (up to 520 footprints per square metre) and frequent overprinting: the footprints are moderately to poorly preserved and may be deeply impressed (up to 2.5 mm deep). There is a gradual transition in preservational quality towards the margins (composed of siltstone), where there are sparse sharp, shallower, well-preserved footprints having distinct pad impressions. This variation in footprint preservation suggests that the substrate in the central area of the trampled horizons was more watery than the marginal areas. Sedimentological analysis indicates that the track-bearing sediments were deposited in shallow ponds associated with an ephemeral fluvial system.

Table 1 summarizes the measurements of 50 distinct footprints, including eight tracks (a total of thirty footprints) and twenty isolated footprints (Fig. 1). The tracks are bipedal, displaying high pace angulation and a straight or slightly curved path; they lack a preferred relative orientation (Fig. 1a, b). The footprints frequently show a positive (inward) rotation in relation to the midline, the pace length being 2.4 to 4.5 times the mean footprint length (without hallux); they may be tetradactyl (58%) or tridactyl (42%) and, exclusive of the hallux impression, are consistently wider than their length. Tridactyl and tetradactyl footprints display a similar overall morphology and may be present in the same track; it is thus evident that they were left by the same producer, the hallux imprints not always being preserved. Digit impressions are slender (maximum

Table 1 Summary of measured track and footprint parameters

	Mean	Minimum	Maximum	n
Footprint length*	27.5	18.7	38.6	50
Footprint length†	36.3	29.4	46.3	29
Width	34.6	27.7	42.7	49
Length I	6.4	2	11.4	29
Length II	14.8	10.6	19.7	49
Length III	20.3	14.5	31.7	49
Length IV	17.3	10.9	22.9	48
Angle II–IV	115°	87°	137°	49
Angle II–III	59.5°	36°	74°	49
Angle III–IV	56.9°	35°	77°	49
Angle I–III	160°	133°	180°	28
Pace angulation	166.2°	107.5°	178°	15
Stride length	193.1	137	245	14
Departure midline	10.9°	0°	29°	29
Length/width	0.80	0.65	0.91	49
I/III‡	0.31	0.13	0.73	29
II/III‡	0.74	0.45	0.98	49
IV/III‡	0.87	0.49	1.31	48

All linear measurement in millimetres.
*Length without hallux. †Length including hallux. ‡Digit impression length ratios.
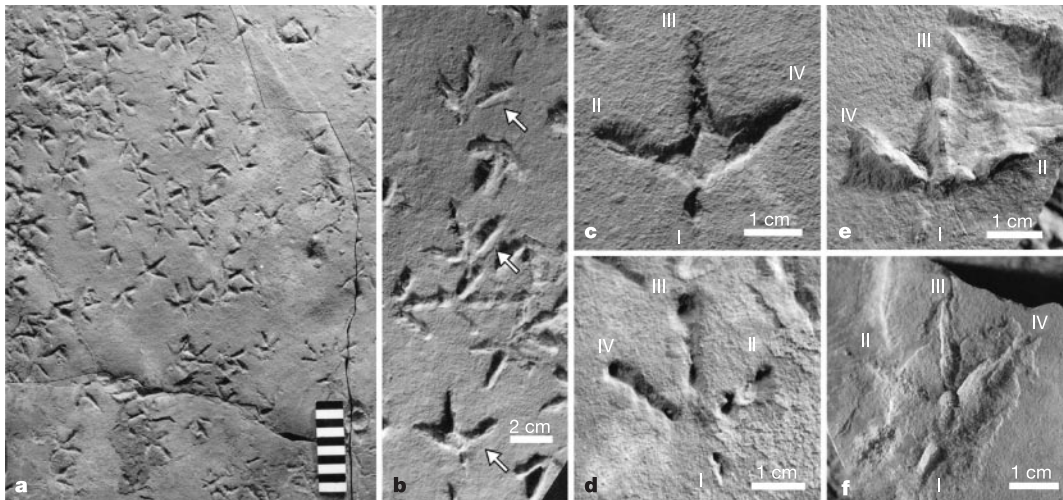
Figure 1 Late Triassic bird-like footprints from the Santo Domingo Formation. **a**, View of part of the lower trampled horizon, showing footprints preserved as natural moulds. Note an increase in footprint density at the upper left of the photo. Scale, 10 cm. **b**, Detailed view of a track preserved as a natural cast and composed of three tetradactyl footprints (arrowed). Note the high pace angulation and rotation of foot axis toward the midline. **c**–**f** Close-up of four footprint preservational variants, as natural moulds (**c**,**d**) and casts (**e**,**f**). All footprints except **e** correspond to the left hind limb. I to IV refer to first to fourth digit imprints. **c**, Deeply imprinted footprint lacking pad impressions (note remains of matrix within the footprint). **d**, Footprint with well-defined pad impressions and rounded ends of digit prints II to IV. Digit I shows claw mark and a single pad impression. **e**, Footprint with pad impressions, small rounded sole, distal curvature of lateral and medial claw marks away from the foot axis, and shallow hallux impression. Part of a second footprint is shown in the upper right corner. **f**, Probable undertrack that exhibits an elliptical sole and a moderately large hallucal impression. Lighting is from the top except for **b**, illuminated from the bottom.

width, 4 mm) and may display a tapered or subparallel outline. The proximal ends of the digit impressions may converge into a conspicuous rounded or elliptical sole (Fig. 1e,f). When present, phalangeal pad impressions are distinct (Fig. 1f) and always display the relation 2-3-4-5 (impressions of toes I-II-III-IV). Toe impressions usually bear slim claw marks, although rounded digit ends have also been recorded. Claw marks in toes II and IV diverge away from the foot axis, whereas that of digit III is parallel to it or curved inward (Fig. 1c,e). Print of digit III is the longest, with those of digits IV, II and I following in decreasing order of length. Divarication of the impression of digits II–IV is high and the angle between the impression of digits II and III is 2°–3° larger, on average, than the angle between the impression of digits III–IV (Fig. 1). The hallux impression is short, thin, usually faint and set at a high angle to digit III (average 160°), usually 2 mm to 8 mm behind the sole or proximal end of digit III; hallux impressions are clearer in the more deeply imprinted tracks than in the shallower tracks. There is no indication of webbing between the digits.

Different criteria have been suggested to distinguish between the footprints of avian and non-avian theropods[7,8,18–22]. The Santo Domingo tracks described herein meet most proposed features that characterize bird footprints, including (see Fig. 1 and Table 1): (1) an overall similarity to modern bird footprints; (2) footprints that are wider than they are long (not considering the hallux) and of small size; (3) slender digit impressions; (4) a wide angle between digits II and IV; (5) a posterior or posteromedial hallux impression, visible both in shallow and deep tracks; (6) slender claws showing distal curvature of lateral and medial claws away from the foot axis; and (7) a sole or metatarsal–phalangeal impression is visible in some footprints, where digits II to IV converge. Additional indications of an avian affinity are afforded by comparison with tracks of modern waterbirds and waders[19,21]; these are: (8) high footprint density and absence of preferred orientation; and (9) occurrence in a shallow lacustrine setting, an environment where bird tracks are preferentially preserved. Although these avian features can be found in isolation and, exceptionally, in non-avian footprints, their combined occurrence in the studied track assemblage is exclusive to birds[2,18,20,22]. This conclusion is supported by the study of a relatively large sample size of footprints preserved in substrates of different consistency, and not merely by single footprints or short tracks[2,3].

Features not in agreement with an avian origin for these bird-like tracks are less significant; they include the presence of distinct pad impressions in some footprints and the absence of associated feeding traces[19]. The shallow hallucal impression, commonly disconnected with the rest of the foot, suggests that the hallux contacted the ground, but that it was slightly raised and probably not adapted for perching as in some birds (compare with ref. 7). In addition, divarication of digits II–IV in tridactyl non-avian dinosaur footprints may reach high values in a few cases, and high pace angulation is not exclusive to birds[2,20].

Bird-like footprints are rare in the Mesozoic era record and occur predominantly in Cretaceous period strata[19,23]. Pre-Cretaceous evidence is more sparse and can be traced back to the Early Jurassic[1,3,4,20,24]. For the Triassic period, it has been suggested that some described ichnogenera (mainly *Plesiornis* and *Trisauropodiscus*) might be likewise "aviform" to varying degrees[1,19,24–26]. However, these footprints show few avian characters and are not comparable with the footprints described herein. *Plesiornis* footprints show low divarication between the impression of digits II and IV (61°–92°), a U-shaped outline, and relatively thick digit imprints[8], features that contrast with typical bird footprints. The poorly preserved[9] Triassic specimens of *Trisauropodiscus* are similar to *Anomoepus*[8,9]; however, that ichnogenus is believed to be the product of an ornithischian trackmaker[1,8,9].

Whatever the ichnotaxonomic affinities of these footprints, their producers are unknown from Late Triassic skeletal remains. In particular, the Late Triassic theropodan record is sparse[27] and no theropod shows evidence of an avian-like reversed hallux[7]. Consequently, these bird-like footprints can only be attributed to an unknown group of theropods showing some avian characters. □

1. Haubold, H. *Saurierfährten* (Ziemsen, Wittenburg, 1984).
2. Thulborn, R. A. *Dinosaur Tracks* (Chapman & Hall, London, 1990).
3. Lockley, M. G. & Hunt, A. P. *Dinosaur Tracks and Other Fossil Footprints of the Western United States* (Columbia Univ. Press, New York, 1995).
4. Lockley, M. G. & Meyer, C. *Dinosaur Tracks and other Fossil Footprints of Europe* (Columbia Univ. Press, New York, 2000).
5. Ostrom, J. H. Bird flight, how did it begin? *Am. Sci.* **67,** 46–56 (1979).
6. Padian, K. & Chiappe, L. M. The origin and early evolution of birds. *Biol. Rev.* **73,** 1–42 (1998).
7. Gatesy, S. M., Middleton, K. M., Jenkins, F. A. & Shubin, N. H. Three-dimensional preservation of foot

movements in Triassic theropod dinosaurs. *Nature* **339**, 141–144 (1999).

8. Gierliński, G. Avialian theropod tracks from the Early Jurassic strata of Poland. *Zubia* **14**, 79–87 (1996).
9. Rainforth, E. C. Late Triassic–Early Jurassic dinosaur ichnofaunas, eastern North America and Southern Africa. *J. Vert. Paleo.* **21**, 91A (2001).
10. Chiappe, L. M. The first 85 million years of avian evolution. *Nature* **378**, 349–355 (1995).
11. Caminos, R., Zamuner, A. B., Limarino, O. C. & Fauqué, L. El Triásico superior fosilífero en la Precordillera riojana. *Rev. Asoc. Geol. Arg.* **50**, 262–265 (1995).
12. Coughlin, T. J. *Linked Orogen-Oblique Fault Zones in the Central Argentine Andes: The Basis of a New Model for Andean Orogenesis and Metallogenesis* PhD thesis (Univ. Queensland, 2001).
13. Caminos, R. & Fauqué, L. Geologic sheet 2969-II Tinogasta (1:250,000). *Ser. Geol. Min. Arg.* (2001).
14. Artabe, A. E., Brea, M. & Zamuner, A. B. *Rhexoxylon brunoi* Artabe, Brea et Zamuner, sp. nov., a new Triassic Corystosperm from the Paramillo de Uspallata, Mendoza, Argentina. *Rev. Palaeobot. Palyn.* **105**, 63–74 (1999).
15. Gradstein, F. M. *et al.* A Triassic, Jurassic and Cretaceous time scale. *SEPM Spec. Publ.* **54**, 95–126 (1995).
16. Kent, D. V. & Olsen, P. E. Implications of astronomical climate cycles to the chronology of the Late Triassic. *Zbl. Geol. Paläont.* **8**, 1463–1473 (2000).
17. Pálfy, J., Smith, P. L. & Mortensen, J. K. A U-Pb and ^{40}Ar/^{39}Ar time scale for the Jurassic. *Can. J. Earth Sci.* **37**, 923–944 (2000).
18. Currie, P. Bird footprints from the Gething Formation (Aptian, Lower Cretaceous) of northeastern British Columbia, Canada. *J. Vert. Paleontol.* **1**, 257–264 (1981).
19. Lockley, M. G., Yang, S-Y., Matsukawa, M., Fleming, F. & Lim, S-K. The track record of Mesozoic birds: evidence and implications. *Phil. Trans. R. Soc. Lond. B* **336**, 113–134 (1992).
20. Fuentes Vidarte, C. Primeras huellas de aves en el Weald de Soria (España). Nuevo icnogénero, *Archaeornithipus* y nueva icnoespecie. *A. meijidi. Est. Geol.* **52**, 63–75 (1996).
21. Doyle, P., Wood, J. L. & George, G. T. The shorebird ichnofacies: an example from the Miocene of southern Spain. *Geol. Mag.* **137**, 517–536 (2000).
22. McCrea, R. T. & Sarjeant, W. A. S. in *Mesozoic Vertebrate Life* (eds Tanke, D. H. & Carpenter, K.) 453–478 (Indiana Univ. Press, Bloomington/Indianapolis, 2001).
23. Lockley, M. G. The vertebrate track record. *Nature* **396**, 429–432 (1998).
24. Ellenberger, P. Contribution à la classification des pistes de vertébrés du Trias: Les types du Stormberg d'Afrique du Sud (I). *Palaeovert. Mém. Extraordinaire*, 1–128 (1972).
25. Weems, R. E. & Kimmel, P. G. Upper Triassic reptile footprints and a coelacanth fish scale from the Culpeper basin, Virginia. *Proc. Biol. Soc. Wash.* **106**, 390–401 (1993).
26. Gierlinski, G. & Sabath, K. Protoavian affinity of the *Plesiornis* trackmaker. *J. Vert. Paleo.* **18**, 46A (1998).
27. Heckert, A. B. & Lucas, S. G. Global correlation of the Triassic theropod record. *Gaia* **15**, 63–74 (1998).

Overlap of internal models in motor cortex for mechanical loads during reaching

Paul L. Gribble* & **Stephen H. Scott**

Department of Anatomy and Cell Biology, CIHR Group in Sensory-Motor Systems, Centre for Neuroscience Studies, Queen's University, Kingston, Ontario K7L 3N6, Canada

A hallmark of the human motor system is its ability to adapt motor patterns for different environmental conditions, such as when a skilled ice-hockey player accurately shoots a puck with or without protective equipment. Each object (stick, shoulder pad, elbow pad) imparts a distinct load upon the limb, and a key problem in motor neuroscience is to understand how the brain controls movement for different mechanical contexts[1,2]. We

* Present address: Department of Psychology, The University of Western Ontario, London, Ontario N6A 5C2, Canada

addressed this issue by training non-human primates to make reaching movements with and without viscous loads applied to the shoulder and/or elbow joints, and then examined neural representations in primary motor cortex (MI) for each load condition. Even though the shoulder and elbow loads are mechanically independent, we found that some neurons responded to both of these single-joint loads. Furthermore, changes in activity of individual neurons during multi-joint loads could be predicted from their response to subordinate single-joint loads. These findings suggest that neural representations of different mechanical contexts in MI are organized in a highly structured manner that may provide a neural basis for how complex motor behaviour is learned from simpler motor tasks.

Behavioural studies suggest that the brain uses internal models—neural processes that mimic the characteristics of the body or environment—to predict and generate motor commands for movement[1,3], but little is known about neural computations associated with these representations[4,5]. Here we test two qualitatively distinct hypotheses about the organization in the brain of internal models for different mechanical loads[2]. One possibility is that internal models for different loads are represented within a single controller that encapsulates all possible loads (Fig. 1a). A second possibility is a more modular scheme in which multiple controllers co-exist, each suitable for one context (or a small set of contexts) (Fig. 1b). These two hypotheses predict differences in how individual neurons in the brain respond when loads are applied in a given motor task: either a cell consistently changes activity for all mechanical loads (former), or it changes activity only for one or a subset of loads (latter). We tested these two alternatives using a reaching task with different dynamic loads, and recorded neuronal activity in MI, a region intimately involved in volitional motor control where cells often respond to changes in force output[4–8].

We trained monkeys to wear a robotic exoskeleton (KINARM) that permitted horizontal limb movements using flexion and extension motions at the shoulder and elbow[9,10]. Monkeys made reaching movements without loads (NL) and with one of three
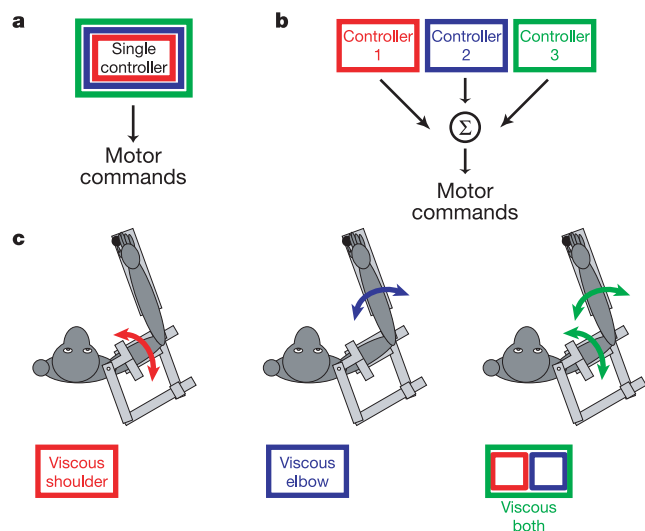
Figure 1 Two hypotheses about the neural control of different mechanical loads. A single-controller that encapsulates all load contexts (**a**), or multiple controllers, each of which represent individual loads (**b**). **c**, Experimental design used to assess the neural representation of multiple loads. A robotic exoskeleton applied velocity-dependent (viscous) loads to the monkey's arm during reaching movements. Viscous shoulder (VS) and viscous elbow (VE) are mechanically independent loads. Viscous both (VB) is the superposition of viscous shoulder and viscous elbow loads.